An Improved Solution Structure for ψ-Conotoxin PIIIE[†,‡]

Ryan M. Van Wagoner[§] and Chris M. Ireland*

Department of Medicinal Chemistry, University of Utah, Salt Lake City, Utah 84112

Received December 2, 2002; Revised Manuscript Received March 25, 2003

ABSTRACT: A revised, high-resolution structure of ψ-conotoxin PIIIE (ψ-PIIIE), a noncompetitive inhibitor of the nicotinic acetylcholine receptor (nAChR), produced through the use of NMR and molecular modeling calculations is presented. The original structures of ψ-PIIIE had a relatively high degree of disorder, particularly in the conformation of the disulfide bridges. Our studies utilized ^{13}C-labeling of selected cysteine residues allowing the resolution of all problems of resonance overlap for the cysteine residues. The improved data were used to produce a new set of structures by a molecular modeling process incorporating relaxation matrix methods for the determination of interproton distance restraints and a combination of distance geometry and simulated annealing for structure generation. The structures produced are very well converged with the RMSD of backbone atom positions of the main body of the peptide improving from 0.73 to 0.13 Å. Other indicators of correlation with the experimental data and quality of covalent geometry showed significant improvement in the new structures. The overall conformation of the peptide backbone is similar between the two determinations with the exception of the N-terminus. This difference leads to a significant effect on the predicted distribution of positive charge within ψ-PIIIE, a property likely to influence interpretation of future mutational studies.

ψ-Conotoxin PIIIE (ψ-PIIIE; Figure 1)[1] is a noncompetitive antagonist of skeletal nicotinic acetylcholine receptors (nAChR) isolated from a Gulf of California specimen of the pisciverous cone snail *Conus purpurascens*. We have recently determined the three-dimensional structure of ψ-PIIIE through the use of NMR in the determination of distance restraints (*1*). The results of the calculations were an ensemble of 14 structures

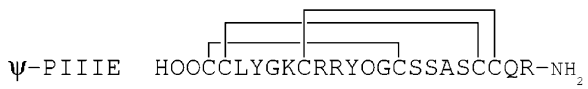

FIGURE 1: Sequence of ψ-conotoxin PIIIE. O = *trans*-4-hydroxyproline; -NH_2 = amidated C-terminus.

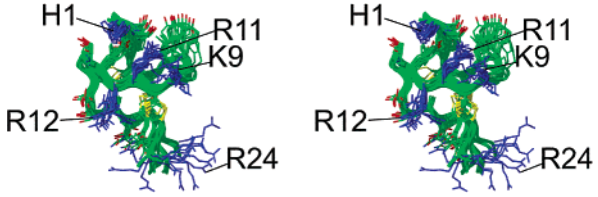

FIGURE 2: Original structures calculated for ψ-conotoxin PIIIE by Mitchell et al. Defocused stereoview showing the backbone as a ribbon with the heavy atoms of side chains shown as well. The side chains of basic residues are colored blue.

(PDB ID 1AS5, Figure 2) that had the same three-dimensional disulfide bridge topology as the voltage sensitive sodium channel inhibitory μ-conotoxins, peptides having a similar pattern of occurrence of cysteine residues and disulfide bridge pairing. The models exhibited a significant degree of disorder associated not only with the terminal ends of ψ-PIIIE, but also with many areas of the backbone within the main body of the peptide. We raised the question as to whether the disorder was indicative of structural dynamics for ψ-PIIIE or whether it resulted from a paucity of NMR data caused by resonance overlap. One interesting aspect of the structures calculated for ψ-PIIIE was the amount of disorder in disulfide bridge conformation. The one bridge that was somewhat well-converged (Cys4−16) was the only bridge for which cross-disulfide distance restraints had been determined. For most other cysteine residues, overlap of crucial cross-peaks indicative of $^3J_{H\alpha H\beta}$ or of intraresidue

[†] This work was supported by an NIH fellowship (GM08573) to R.M.V., by an American Foundation for Pharmaceutical Education predoctoral fellowship to R.M.V., and by an American Chemical Society Division of Medicinal Chemistry predoctoral fellowship funded by Pfizer to R.M.V.

[‡] Atomic coordinates for the 13 converged structures of ψ-PIIIE have been deposited in the Protein Data Bank for release upon publication (accession code 1JLO).

* Corresponding author. Tel: (801) 581−8305. Fax: (801) 581−6208. E-mail: cireland@deans.pharm.utah.edu.

[§] Current Address: Department of Biological Chemistry and Molecular Pharmacology, Harvard Medical School, 250 Longwood Ave., Boston, MA 02115, USA.

[1] Abbreviations: ψ-PIIIE, ψ-conotoxin PIIIE; O, *trans*-4-hydroxyproline; nAChR, nicotinic acetylcholine receptor; NMR, nuclear magnetic resonance; fmoc, fluorenylmethoxycarbonyl; GSH, reduced form of glutathione; GSSG, oxidized form of glutathione; C_{18} HPLC, octadecylsilyl reversed-phase high-performance liquid chromatography; CH_3-CN, acetonitrile; TFA, trifluoroacetic acid; MALDI-MS, matrix-assisted laser desorption ionization mass spectrometry; D_2O, deuterium oxide; TOCSY, total correlation spectroscopy, DQF−COSY, double quantum filtered correlation spectroscopy; NOESY−HSQC, three-dimensional nuclear Overhauser effect spectroscopy/heteronuclear single quantum coherence spectroscopy; fHSQC, fast heteronuclear single quantum coherence spectroscopy; NOESY, nuclear Overhauser effect spectroscopy; PECOSY, primitive exclusive correlation spectroscopy; WET, water suppression enhanced through T_1 effects; WATERGATE, water suppression by gradient-tailored excitation; I-BURP, inverting band-selective uniform response pure phase pulse; FID, free induction decay; DGII, distance geometry II; IRMA, iterative relaxation matrix approach; CVFF, constant valence force field; nOe, nuclear Overhauser effect; RMSD, root-mean-squared deviation.

10.1021/bi027274e CCC: $25.00
Published on Web 05/07/2003

distance restraints prevented determination of restraints on χ^1. Thus, it was impossible to determine whether the side chains of the cysteine residues are rotationally static or dynamic.

We postulated that greater resolution of the molecular model could be achieved if restraints on χ^1 were determined for all cysteine residues, thus potentially elucidating whether the side chains of the cysteine residues are rotationally static or dynamic. Interestingly, based on analysis of deposited conotoxin structures in the Protein Data Bank (*2*) for which multiple independent structural determinations have been undertaken, the appearance of heterogeneity in disulfide bridge conformation often results from having insufficient data to distinguish between the alternate conformers rather than from any actual dynamic motion of the disulfide bridges (*3*). There have been cases, however, where experimental observations indicate that dynamic fluctuation of disulfide bridge conformation may indeed be taking place under the experimental conditions (*4*−*6*). To explore the conformation of cysteine residues in ψ-PIIIE, we used chemical synthesis to produce ψ-PIIIE containing 3-^{13}C-labeled cysteine at selected positions in the sequence in such a way as to allow resolution of all ^{1}H NMR overlap problems for the cysteine residues of ψ-PIIIE. We were able to collect an improved data set containing a large number of restraints on interproton distances and torsion angles that were applied to molecular modeling calculations to produce a new set of structures of ψ-PIIIE. The use of a more extensive data set led to significant improvement over the structures originally reported for ψ-PIIIE in a number of parameters describing structural quality.

EXPERIMENTAL PROCEDURES

Peptide Synthesis. 99% [3-^{13}C]-*N*-(9-fluorenylmethoxycarbonyl)-*S*-trityl-L-cysteine was synthesized as previously described (*7*, *8*) using 99% [3-^{13}C]-L-cysteine (Cambridge Isotope Laboratories, CLM-1868). The labeled amino acid was incorporated into positions C4 and C21 of ψ-PIIIE using fmoc-based solid-phase chemical synthesis (50 μmole scale) (*9*). The ^{13}C-labeled residues were reacted with the resin at a 5-fold excess and the natural isotopic abundance residues were reacted at a 10-fold excess. All cysteine residues were incorporated as trityl thioether derivatives and the side chains of other residues were protected as previously described (*10*). Deprotection and purification of the peptide were achieved using a procedure similar to that originally used for the synthesis of ψ-PIIIE (*11*). Disulfide bridge formation was achieved by incubation of linear peptide in a 0.1 M pH 7.7 phosphate buffer solution containing 1.0 mM GSH and 0.5 mM GSSG for 12−16 h at room temperature. The major folded product isolated by preparative C_{18} HPLC was found to coelute with authentic ψ-PIIIE using a 10−60% gradient of 60% CH_3CN, 0.092% TFA in 0.1% TFA over 50 min on analytical C_{18} HPLC. MALDI-MS indicated an average molecular mass of 2720.77 Da (calculated 2720.2 Da). The total yield from 200 mg of resin was 14.1 mg of peptide (4.14 μmol of the hexa-TFA salt of ψ-PIIIE).

NMR Data Acquisition. For NMR studies, 14.1 mg of peptide were dissolved in 260 μL of a 9:1 water/D_2O solution to provide a solution roughly 16 mM in concentration. The pH of the solution was adjusted to 3.48 with dilute TFA prior to addition of the peptide. For studies requiring observation of peaks with resonance frequencies similar to water, 14.1 mg of lyophilized peptide were dissolved in 260 μL of D_2O. The solution conditions for NMR data acquisition were chosen to be similar to those used for the original structure determination of ψ-PIIIE.

NMR spectra were acquired on a Varian INOVA 600 MHz NMR spectrometer. Experiments were acquired using a Nalorac triple-resonance gradient-capable probe. A 5-mm NMR microtube with insert matched to D_2O (Shigemi Co., Ltd.) was used for all experiments. The pulse sequences used for TOCSY (*12*), DQF−COSY (*13*), NOESY−HSQC (*14*), and fHSQC (*15*) were similar to those previously described. Pulse sequences for NOESY (*16*) and PECOSY (*17*) experiments were converted to doubly ^{13}C-filtered variants through insertion of appropriate sequences prior to each detection period (*18*). One-dimensional ^{13}C-edited ^{1}H NMR spectra were obtained by using a modified double pulsed field gradient selective excitation (*19*) strategy. A modified form of WET (*20*) water suppression was used for the TOCSY, DQF−COSY, and doubly ^{13}C-filtered NOESY. Water suppression was applied prior to frequency labeling for TOCSY and DQF−COSY and during the mixing time for NOESY spectra. A WATERGATE based methodology (*21*) utilizing a 3919 sequence was used for water suppression of the NOESY−HSQC, and fHSQC experiments. PECOSY and ^{13}C-edited ^{1}H NMR spectra were acquired in D_2O, negating the need for water suppression. Quadrature discrimination of frequencies in the indirectly detected dimension was achieved in all experiments through use of States hypercomplex acquisition (*22*). Unless noted otherwise, the spectral width was 6600 Hz for ^{1}H dimensions and 2000 Hz for ^{13}C dimensions. For the TOCSY and DQF−COSY experiments, a total recycle time of 2.31 s was used with 16 scans each consisting of 2048 complex points. A total of 512 complex points in t_1 were acquired and the acquisition temperature was 4 °C. A mixing time of 80 ms was used for the TOCSY experiment. Parameters were similar for the doubly ^{13}C-filtered NOESY spectra except 32 scans were acquired, the recycle time was 1.510 s, and mixing times of 100, 200, and 400 ms were used. For the NOESY−HSQC, 64 points were acquired in t_1, 128 points in t_2, and 1024 points in t_3. The recycle time was 0.605 s and four transients were acquired. The spectra were acquired at 4 °C with a mixing time of 150 ms. For the fHSQC 128 complex points in t_1 and 2048 complex points in t_2 were acquired with a recycle time of 1.01 s. Four transients were acquired and the temperature of acquisition was 4 °C. The PECOSY experiment was acquired at a temperature of 22 °C with a recycle time of 2.62 s. A total of 512 complex points were acquired in t_1 while 4096 points were acquired in t_2. Thirty-two scans were acquired for each t_1 time point. The ^{13}C-edited ^{1}H NMR spectrum was acquired on a Varian UNITY 500 MHz spectrometer using a Nalorac triple resonance gradient-capable probe. A shaped I-BURP (*23*) pulse pattern having 8.3 ms duration was used for selective inversion of the carbon whose protons were to be observed. A spectral width of 4629 Hz was used and 8192 complex points were collected. The data were acquired at 4 °C.

Data Processing. All NMR data sets were analyzed using either VNMR (Varian, Inc.) or FELIX (Accelrys, Inc). TOCSY, DQF−COSY, and NOESY experiments were zero-

filled once in D1 and three times in D2 to give final matrixes consisting of 4096 by 2048 real points with resolution values of 1.4 and 2.8 Hz/pt for the D1 and D2 vectors, respectively. For NOESY and TOCSY spectra, t_2 FIDs and t_1 interferograms were processed by convolution with 90° phase-shifted sinebell squared curves (with widths of 2048 and 1024 points, respectively) prior to complex fast Fourier transformation. DQF−COSY spectra were processed with 60° phase-shifted sinebell squared curves in t_2 (2048 point width) and t_1 (1024 point width) prior to transformation. The PECOSY data set was processed by zero-filling once in D1 and three times in D2 to give a final matrix of 8192 by 2048 real points and resolution values of 0.7 and 2.8 Hz/pt for the D1 and D2 vectors. Apodization and resolution enhancement were achieved by convolution with 60° phase-shifted sinebell window functions with widths of 4096 points (in t_2) and 512 points (in t_1) prior to transformation. Baseline correction was applied in both dimensions of NOESY and TOCSY experiments to enhance detection of cross correlations and increase the accuracy of volume measurement. Automatic baseline detection was achieved by use of the FLATT algorithm (*24*) with default parameters as provided by FELIX.

Determination of Restraints and Molecular Modeling. All calculations were performed using the Insight II 97.0 suite of programs (Accelrys, Inc). Molecular dynamics calculations were performed using DISCOVER 2.98 (Accelrys, Inc), while DGII 97.0 (Accelrys, Inc.) was used for distance geometry calculations. Distance restraints for the highest quality NOESY cross-peaks were calculated using standard IRMA (Accelrys, Inc.) methodology (*25*, *26*). Lower and upper bound distance restraints from lower quality cross-peaks in NOESY spectra for ψ-PIIIE were respectively set at 90 and 120% of the distance calculated from the isolated spin pair approximation for data collected with a mixing time of 0.100 s. The dihedral angle ϕ was restrained to values of −90° to −40° for $^3J_{HNH\alpha} < 5$ Hz and to the range −160° to −80° for $^3J_{HNH\alpha} > 8$ Hz (*27*). Restraints on χ^1 were restricted to be ±15° of the values determined according to the method of Hyberts et al. (*28*). The pairing of disulfide bonds had been determined experimentally previously (*11*) and were enforced as explicit covalent bonds prior to metric matrix calculations within Insight II. The final structures were generated by distance geometry calculations followed by simulated annealing and energy minimization using standard protocols (*1*, *29*). CVFF Provided all empirical potential energy terms (*30*). The 50 structures generated by this methodology were analyzed on the basis of residual violations of dihedral angle and distance restraints and by potential energy calculations. The force constants were set to values of 20.00 kcal (mol Å^2)$^{-1}$ for all distance restraints and 30.00 kcal (mol radian^2)$^{-1}$ for dihedral angle restraints. Electrostatic potentials were disregarded for all modeling calculations due to the use of in vacuo conditions. The figures were generated using the program MOLMOL 2k.2 (*31*) in conjunction with the POV−Ray rendering program.

RESULTS

Resolution of Data Overlap for Cysteine Residues. For ψ-PIIIE a selective ^{13}C-labeling approach was taken as a means of resolving overlap problems. The two cysteine residues with β proton resonance signals involved in most of the overlap problems in the original data set of ψ-PIIIE (C4 and C21) were labeled, thus removing all overlap problems for C5, C10, and C22 by using isotopic filtering. The use of ^{13}C-labeling also allowed the application of ^{13}C-editing approaches to further resolve the overlap problems between C4 and C21, providing that the ^{13}C chemical shifts were sufficiently well resolved between the two residues. Incorporation of cysteine labeled with ^{13}C at C$^\beta$ by solid phase chemical synthesis was selected as the most straightforward approach likely to provide the desired information given reactant availability and the specific overlap problems present. Selective ^{13}C-labeling of C4 and C21 provided additional advantages over selective ^{13}C-labeling of all cysteine residues. The likelihood of overlap for ^{13}C chemical shift was greatly reduced with only two residues labeled compared to five or six. Also, smaller amounts of the expensive ^{13}C-labeled cysteine reagent were required for labeling of only two residues.

Measurement of intraresidue nOe coupling interactions for C4 and C21 was achieved through the use of a three-dimensional NOESY−HSQC. Separate NOESY spectra for C4 and for C21 were produced by taking two-dimensional slices at the chemical shift of the respective carbons. The method decided upon for determination of $^3J_{H\alpha H\beta}$ for C4 and C21 was direct measurement of $^3J_{H\alpha H\beta}$ from the multiplet structure observed in a ^{13}C-selected one-dimensional ^{1}H NMR spectrum. Fortunately, the line widths of ψ-PIIIE are narrow enough to allow measurement of $^3J_{H\alpha H\beta}$ as small as 3−4 Hz. Because of the overlap of C4H$^{\beta H}$ and C21H$^{\beta L}$, however, it was necessary to develop an approach that allowed selective observation of H$^\beta$ for C4 and C21 separately. This was achieved using a gradient-selected ^{13}C to ^{1}H polarization transfer experiment (see Supporting Information for a pulse diagram). Variants of NOESY and PECOSY experiments were designed to incorporate ^{13}C-filtering elements at either or both of the ^{1}H detection periods, thus allowing ^{13}C-filtering of signals in either or both dimensions of the experiments (see Supporting Information). Measurement of $^3J_{H\alpha H\beta}$ and the intraresidue H^N:H$^\beta$ and H$^\alpha$:H$^\beta$ nOe cross-peak volumes from these filtered experiments provided information on both the conformation and dynamics associated with χ^1 for the nonlabeled cysteine residues.

Assignment of ^{1}H Resonances, Determination of Restraints on Dihedral Angle, and Stereospecific Assignment. Assignments were made for all observed ^{1}H resonances according to the methodology of Wüthrich (*32*). Restraints on χ^1 were determined for H1, C4, C5, L6, Y7, C10, Y13, C16, S18, S20, C21, C22, and Q23 based on $^3J_{H\alpha H\beta}$ and on intraresidue H^N:H$^\beta$ and H$^\alpha$:H$^\beta$ nOe interactions (*28*). This analysis also allowed the determination of stereospecific restraints for the prochiral side chain hydrogen atoms of residues C4, C5, L6, Y7, C10, R12, Y13, C16, S18, S20, C21, C22, and Q23. Additionally, analysis of the pattern of intraresidue nOe interactions for hydroxyproline residues (*1*) led to stereospecific assignment of all prochiral hydrogen atoms of residues O2, O3, and O14. Restraints on ϕ were determined from measurement of $^3J_{HNH\alpha}$ according to previously described methods (*33*). The intraresidue and sequential nOe interactions measured were not indicative of regular α-helical or β-strand structures in ψ-PIIIE.

Structure Calculations and Evaluation for ψ-PIIIE. A total of 524 distance restraints were derived from the NOESY data through either relaxation matrix calculations (*25*, *26*)

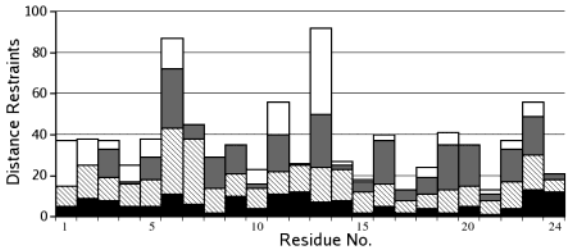

FIGURE 3: Distribution of distance restraints across the sequence of ψ-PIIIE. Black bars indicate intraresidue restraints, crosshatched bars indicate sequential restraints, gray bars indicate restraints between residues separated by 2−4 amino acids, and white bars indicate long-range distance restraints.

Table 1: Structural Statistics for the Revised and Original Structures of ψ-Conotoxin PIIIE

	revised structures	original structures
RMSD for C^{α}, N, C atoms from average molecule coordinates (Å)		
residues 4−22	0.13	0.73
all residues	0.22	0.91
RMSD from distance restraints (Å)	0.140	0.130
RMSD from dihedral restraints (deg)	2.34	3.03
R_1 for ensemble	0.350	0.597
RMSD from idealized geometry		
bond lengths (Å)	0.0142 ± 0.002	0.0185 ± 0.004
bond angles (deg)	2.67 ± 0.02	3.6 ± 0.2
energies (kcal mol^{-1})		
$E_{restraint}$	224 ± 5	190 ± 20
E_{L-J}	189 ± 3	300 ± 20
$E_{bond} + E_{angle} + E_{improper}$	298 ± 5	460 ± 30
Ramachandran plot statistics (%)		
residues in most favored region	78	55
residues in additionally allowed region	22	37
residues in generously allowed region	0	8
residues in nonallowed region	0	0.4

or estimations based on the isolated spin pair approximation (*34*) for cross-peaks in the 100 ms NOESY spectrum (Figure 3). The restraints on interproton distances and dihedral angles were used as input for molecular modeling calculations based on combined use (*29*) of distance geometry II (DGII) (*35*) and simulated annealing to generate a set of 50 structures. Thirteen of the 50 structures were found to converge by analysis of residual restraint violations and energy calculations. The ensemble of structures calculated for ψ-PIIIE shows good convergence of backbone atom coordinates (see Table 1). An overall RMSD of 0.22 Å is found for all residues with that figure decreasing to 0.13 Å for the main body of the peptide between residues 4 and 22. The side chains of most residues are also reasonably well-converged with only K9, R12, and R24 showing high degrees of disorder and R11 showing a somewhat smaller amount of heterogeneity of structure. The stereochemistry for the models of ψ-PIIIE is reasonably consistent with expected peptide geometry. Overall, 78% of residues occur in the most favored regions identified by Ramachandran analysis (*36*) while 22% occur in additionally allowed regions of the plot as determined by the program PROCHECK_NMR (*37*). One recent report has noted that small disulfide-rich proteins tend to score poorly by stereochemical analysis of the type reported above, possibly due to strain associated with the tightly constrained structures (*38*). The structures also showed low RMSD from ideal bond lengths and bond angles, indicating that satisfaction of the experimental restraints on structure does not require significant distortion of covalent geometry.

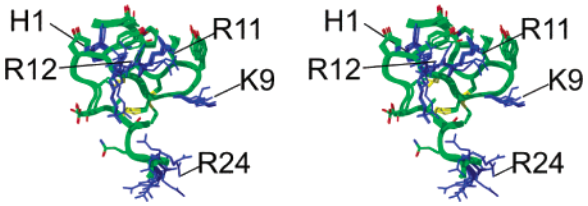

FIGURE 4: Defocused stereoviews of the 13 converged structures of ψ-PIIIE produced by simulated annealing calculations. All structures are aligned with the N-terminus toward the top of the figure and the C-terminus toward the bottom. Only the heavy atoms of the side chains are shown. The side chains of basic residues are colored blue.

Table 2: Observed Elements of Secondary Structure in the New Structures of ψ-PIIIE

residues	structural element
H1−C4	Type VII β turn
O2−C5	Type VIa β turn
O3−L6	Type VIII β turn
L6−K9	Type I′ β turn
R11−Y13	inverse γ turn
Y13−C16	Type II β turn
C16−A19	Type I β turn
A19−C22	Type III β turn
S20−Q23	Type III β turn
C21−R24	Type III β turn

Three-Dimensional Structure. The converged structures of ψ-PIIIE are illustrated in Figure 4. Like many conotoxins, ψ-PIIIE consists of a compact disulfide core with most noncysteine side chains oriented away from the interior of the peptide. Residues likely to constitute the hydrophobic core of the peptide (indicated by >80% buried surface area as calculated by MOLMOL 2k.2) include C4, C5, L6, Y13, C16, A19, C21, and C22. Residues with >60% solvent exposure include R12 and R24. ψ-PIIIE does not appear to contain any β-sheets longer than two residues. The region between residues 19 and 23 has a roughly α-helical conformation though secondary structure detection by MOLMOL2k.2 indicated helicity for only 1 of the 13 structures. There are, however, a number of reverse turns indicated by the backbone torsion angles and predicted H-bonds in the calculated structures (Table 2 and Supporting Information).

DISCUSSION

Revised Structure of ψ-PIIIE. Overall the structure of ψ-PIIIE is compact and well defined. The main body of the peptide has the rough shape of a shallow trigonal prism; when viewed from the "side" the molecule has a smaller profile than when viewed from the "front" or "back" (see Figure 5). The N-terminus is well-converged with the aromatic side chain of H1 aligned along a face of the peptide. Each of the three disulfide bridges are very well-converged with the sole exception being a single alternate disulfide conformation for the bridge Cys4−16. The structures calculated for ψ-PIIIE do not have either the intercysteine loop spacings nor the three-dimensional disulfide bridge arrangement expected for an inhibitor cystine knot fold (*39*). As was the case for the original structures of ψ-PIIIE, the overall fold bears little similarity to other conotoxins aside from the overall three-

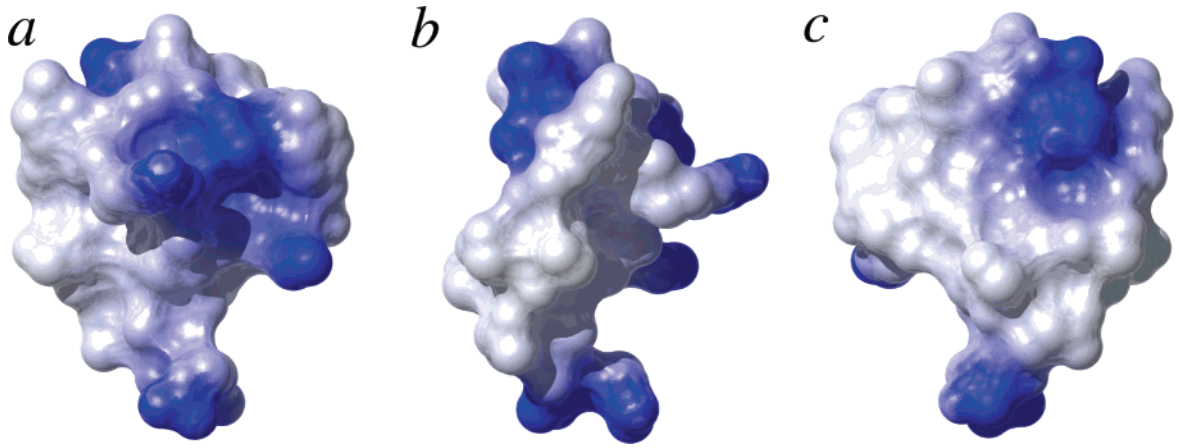

FIGURE 5: The electrostatic surface potential of a representative model of ψ-PIIIE is shown from three different vantage points. Blue regions indicate a positive electric potential. The regions of most intense color correspond to a charge of +1 or greater. Potential calculations were performed using the SimpleCharge algorithm of MOLMOL 2k.2. (a) View from the "front" side of the peptide, or the side of the peptide containing all of the positive charges in the original structure determination of ψ-PIIIE. (b) View from the side of ψ-PIIIE. The front of the peptide corresponds to the right side of the molecule where the side chain of R12 is visible in the upper half of the molecule. (c) The back face of ψ-PIIIE. The side chain of H1 is packed against the top of the molecule in this vantage point.

dimensional arrangement of disulfide bridges in the μ-conotoxins.

There are six positive charges present on ψ-PIIIE at the pH used for NMR studies and these are distributed among three main sites of positive charge density: near residue 1, near residues 9−12, and at residue 24. The positive charges associated with H1 are both located on the rear face of the molecule near the top. Both positively charged moieties are well defined in the structures. The three positive charges occurring at K9, R11, and R12 are located in the upper half of the front of the peptide. Of the three residues, the side chain of R11 appears to be best defined by the data. The side chain of R11 is also the only one of the three to align along the face of the molecule; the side chains of K9 and R12 project perpendicular to the body of the peptide. The side chains of K9 and R12 have a significantly higher degree of solvent exposure than R11 (see Figure 4). The third region of positive charge density occurs at the C-terminus of the peptide. The conformation of the side chain of R24 is more poorly defined than that of any other residue in the peptide.

Comparison with the Original Structures of ψ-PIIIE. Before comparisons between the original and new structures determined for ψ-PIIIE are made, it should be noted that there were a number of improvements made to the restraint set in addition to specification of χ^1 restraints for all cysteine residues. A higher concentration of peptide was used in the new studies (16 mM) compared to the old studies (4.3 mM). There were additional improvements in the quality of water suppression and in magnetic field strength that increased the quality and quantity of restraints on structure that could be determined from the data. A comparison of the restraint sets is given in Table 3. It is therefore not surprising to note that there was significant improvement in a number of parameters indicative of structure quality for the revised structures of ψ-PIIIE (see Table 1). Taken together, these statistics indicate that the new structures of ψ-PIIIE are more precise, less strained, and a better fit to the experimental data than were the original structures. Additionally, the occurrence of apparent shielding effects in some protons is better explained by the arrangement of aromatic rings in the new structures than in the old structures.

Table 3: Comparison of Restraints Used for the Structure Determinations of ψ-PIIIE

	original structures	new structures
distance restraints		
intraresidue	142	154
sequential	99	156
medium	19	131
long	20	83
total	280	524
dihedral restraints		
ϕ	10	9
χ^1	6	13
total	16	22

The backbone conformations in the original and new structures are very similar to each other (compare Figures 2 and 4). The overall paths traversed by the backbones are nearly identical over most of the length of the toxin. Both sets of structures include reverse turns at similar positions (O3−L6, L6−K9, R11−Y13, Y13−C16, C16−A19, and A19−C22). In the original structure determination, however, the N-terminus projects toward the front of the peptide whereas in the new structure determination it projects toward the back. All six of the positive charges in the original structure of ψ-PIIIE are located on the front face of the peptide (see Figure 2), a circumstance indicating that this face of the molecule is important in interacting with the nAChR as the channel contains both cation-binding sites and a cation-conductive channel. In particular, since ψ-PIIIE acts as a noncompetitive inhibitor, it is possible that the toxin-binding site could be near the ion channel where the peptide can sterically block ion conductance. In the new set of structures, however, the two positive charges associated with H1 are actually located on the back face of the peptide (see Figure 5).

The two sets of structures differ in the degree of definition of the conformations of the three disulfide bridges. As was mentioned previously, all three disulfide bridges were poorly defined in the original structure determination of ψ-PIIIE. The disulfide bridges of the new structures, on the other hand, are very well-converged (see Figure 6). This convergence

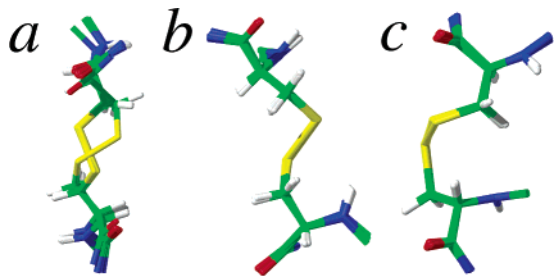

FIGURE 6: The disulfide bridges from the revised structure of ψ-PIIIE with each of the three disulfide bridges overlapped for minimum RMSD. (a) Cys4−16, (b) Cys5−21, (c) Cys10−22.

is well supported by the NMR data as the $^3J_{H\alpha H\beta}$ values and intraresidue distance restraints were all consistent with static and staggered conformations for all six cysteine residues. These results indicate that the conformational heterogeneity observed in the disulfide bridges of the original structures of ψ-PIIIE was caused by inadequacies in the data that prevented determination of reliable restraints on χ^1 for the cysteine residues.

ACKNOWLEDGMENT

We thank Dr. B. M. Olivera for the use of equipment to produce and purify the peptide used in this study. We thank R. G. Dela Cruz and R. B. Jacobsen for guidance in the purification of the peptide and Dr. Robert Schackmann for performing the solid phase synthesis. We also thank the University of Utah Department of Medicinal Chemistry mass spectrometry facility for mass spectral analysis. We thank the University of Utah Health Sciences NMR Facility for assistance in data acquisition. We acknowledge the NIH Grants RR13030, and RR06262 (C.M.I.), and NSF Grant DBI-0002806 for funding NMR instrumentation in the Health Sciences NMR Facility.

SUPPORTING INFORMATION AVAILABLE

One table showing full chemical shift assignments for ψ-PIIIE, the full set of restraints used to calculate the structures, the parameters used for molecular modeling, one table illustrating hydrogen bonds observed in the new models, and one figure illustrating some of the ^{13}C-filtering and editing pulse sequences used in these studies. This material is available free of charge via the Internet at http://pubs.acs.org.

REFERENCES

1. Mitchell, S. S., Shon, K. J., Foster, M. P., Davis, D. R., Olivera, B. M., and Ireland, C. M. (1998) *Biochemistry 37*, 1215−1220.
2. Berman, H. M., Westbrook, J., Feng, Z., Gilliland, G., Bhat, T. N., Weissig, H., Shindyalov, I. N., and Bourne, P. E. (2000) *Nucleic Acids Res. 28*, 235−242.
3. Van Wagoner, R. M. (2001) PhD Dissertation, Department of Medicinal Chemistry, University of Utah, Salt Lake City.
4. Atkinson, R. A., Kieffer, B., Dejaegere, A., Sirockin, F., and Lefevre, J. F. (2000) *Biochemistry 39*, 3908−3919.
5. Rigby, A. C., Lucas-Meunier, E., Kalume, D. E., Czerwiec, E., Hambe, B., Dahlqvist, I., Fossier, P., Baux, G., Roepstorff, P., Baleja, J. D., Furie, B. C., Furie, B., and Stenflo, J. (1999) *Proc. Natl. Acad. Sci. U.S.A. 96*, 5758−5763.
6. Maslennikov, I. V., Sobol, A. G., Gladky, K. V., Lugovskoy, A. A., Ostrovsky, A. G., Tsetlin, V. I., Ivanov, V. T., and Arseniev, A. S. (1998) *Eur. J. Biochem. 254*, 238−247.
7. Bodanszky, M., and Bodanszky, A. (1994) in *The Practice of Peptide Synthesis*, pp 68−69, Springer-Verlag, New York.
8. Atherton, E., and Sheppard, R. C. (1989) in *Solid-Phase Peptide Synthesis*, p 60, IRL Press, New York.
9. Fields, G. B., and Noble, R. L. (1990) *Int. J. Peptide Protein Res. 35*, 161−214.
10. Hopkins, C., Grilley, M., Miller, C., Shon, K. J., Cruz, L. J., Gray, W. R., Dykert, J., Rivier, J., Yoshikami, D., and Olivera, B. M. (1995) *J. Biol. Chem. 270*, 22361−22367.
11. Shon, K. J., Grilley, M., Jacobsen, R. B., Cartier, G. E., Hopkins, C., Gray, W. R., Watkins, M., Hillyard, D. R., Rivier, J., Torres, J., Yoshikami, D., and Olivera, B. M. (1997) *Biochemistry 36*, 9581−9587.
12. Braunschweiler, L., and Ernst, R. R. (1983) *J. Magn. Reson. 53*, 521−528.
13. Rance, M., Sørensen, O. W., Bodenhausen, G., Wagner, G., Ernst, R. R., and Wüthrich, K. (1983) *Biochem. Biophys. Res. Commun. 117*, 479−485.
14. Palmer, A. G., III, Cavanagh, J., Byrd, R. A., and Rance, M. (1992) *J. Magn. Reson. 96*, 416−424.
15. Mori, S., Abeygunawardana, C., Johnson, M. O., and van Zijl, P. C. (1995) *J. Magn. Reson. B 108*, 94−98.
16. Jeener, J., Meier, B. H., Bachmann, P., and Ernst, R. R. (1979) *J. Chem. Phys. 71*, 4546−4553.
17. Mueller, L. (1987) *J. Magn. Reson. 72*, 191−196.
18. Folkers, P. J. M., Folmer, R. H. A., Konings, R. N. H., and Hilbers, C. W. (1993) *J. Am. Chem. Soc. 115*, 3798−3799.
19. Hu, H., and Shaka, A. J. (1999) *J. Magn. Reson. 136*, 54−62.
20. Smallcombe, S. H., Patt, S. L., and Kiefer, P. A. (1995) *J. Magn. Reson. A 117*, 295−303.
21. Piotto, M., Saudek, V., and Sklenar, V. (1992) *J. Biomol. NMR 2*, 661−665.
22. States, D. J., Haberkorn, R. A., and Ruben, D. J. (1982) *J. Magn. Reson. 48*, 286−292.
23. Geen, H., and Freeman, R. (1991) *J. Magn. Reson. 93*, 93−141.
24. Guntert, P., and Wüthrich, K. (1992) *J. Magn. Reson. 96*, 403−407.
25. Boelens, R., Koning, T. M. G., and Kaptein, R. (1988) *J. Mol. Struct. 173*, 299−311.
26. Boelens, R., Koning, T. M. G., van der Marel, G. A., van Boom, J. H., and Kaptein, R. (1989) *J. Magn. Reson. 82*, 290−308.
27. DeMarco, A., Llinás, M., and Wüthrich, K. (1978) *Biopolymers 17*, 617−636.
28. Hyberts, S. G., Marki, W., and Wagner, G. (1987) *Eur. J. Biochem. 164*, 625−635.
29. Nilges, M., Clore, G. M., and Gronenborn, A. M. (1988) *FEBS Lett. 229*, 317−324.
30. Dauber-Osguthorpe, P., Roberts, V. A., Osguthorpe, D. J., Wolff, J., Genest, M., and Hagler, A. T. (1988) *Proteins 4*, 31−47.
31. Koradi, R., Billeter, M., and Wüthrich, K. (1996) *J. Mol. Graphics 14*, 51−55.
32. Wüthrich, K. (1986) *NMR of Proteins and Nucleic Acids*, Wiley-Interscience, New York.
33. Pardi, A., Billeter, M., and Wüthrich, K. (1984) *J. Mol. Biol. 180*, 741−751.
34. Thomas, P. D., Basus, V. J., and James, T. L. (1991) *Proc. Natl. Acad. Sci. U.S.A. 88*, 1237−1241.
35. Crippen, G. M., and Havel, T. M. (1988) *Distance Geometry and Molecular Conformation*, Research Studies Press, Taunton, England.
36. Ramachandran, G. N., and Sasisekharan, V. (1968) *Adv. Protein Chem. 23*, 283−438.
37. Laskowski, R. A., Rullmann, J. A. C., MacArthur, M. W., Kaptein, R., and Thornton, J. M. (1996) *J. Biomol. NMR 8*, 477−486.
38. Martí-Renom, M. A., Stote, R. H., Querol, E., Aviles, F. X., and Karplus, M. (2000) *Proteins: Struct., Funct., Genet. 40*, 482−493.
39. Craik, D. J., Daly, N. L., and Waine, C. (2001) *Toxicon 39*, 43−60.

BI027274E